Biomech Model Mechanobiol (2016) 15:1457–1466
DOI 10.1007/s10237-016-0774-5

ORIGINAL PAPER

A hyperelastic fibre-reinforced continuum model of healing tendons with distributed collagen fibre orientations

M. N. Bajuri[1,3] · Hanna Isaksson[2] · Pernilla Eliasson[4] · Mark S. Thompson[1]

Received: 25 September 2015 / Accepted: 20 January 2016 / Published online: 7 March 2016

Abstract The healing process of ruptured tendons is problematic due to scar tissue formation and deteriorated material properties, and in some cases, it may take nearly a year to complete. Mechanical loading has been shown to positively influence tendon healing; however, the mechanisms remain unclear. Computational mechanobiology methods employed extensively to model bone healing have achieved high fidelity. This study aimed to investigate whether an established hyperelastic fibre-reinforced continuum model introduced by Gasser, Ogden and Holzapfel (GOH) can be used to capture the mechanical behaviour of the Achilles tendon under loading during discrete timepoints of the healing process and to assess the model's sensitivity to its microstructural parameters. Curve fitting of the GOH model against experimental tensile testing data of rat Achilles tendons at four timepoints during the tendon repair was used and achieved excellent fits ($0.9903 < R^2 < 0.9986$). A parametric sensitivity study using a three-level central composite design, which is a fractional factorial design method, showed that the collagen-fibre-related parameters in the GOH model—κ, k_1' and k_2'—had almost equal influence on the fitting. This study demonstrates that the GOH hyperelastic fibre-reinforced model is capable of describing the mechanical behaviour of healing tendons and that further experiments should focus on establishing the structural and material parameters of collagen fibres in the healing tissue.

Keywords Tendon healing · Constitutive model · Fibre-reinforced material · Finite element analysis · Fractional factorial design

✉ Mark S. Thompson
mark.thompson@eng.ox.ac.uk

1 Institute of Biomedical Engineering, Department of Engineering Science, University of Oxford, Oxford, UK

2 Department of Biomedical Engineering, Lund University, Lund, Sweden

3 Faculty of Bioengineering and Medical Sciences, Universiti Teknologi Malaysia, Johor Bahru, Malaysia

4 Department of Clinical and Experimental Medicine, Linköping University, Linköping, Sweden

1 Introduction

Tendon rupture is highly disabling. It is associated with substantial pain, and it may take many months or even years of healing until full function has returned. Numerous studies, both in animal models and in patients, have shown that mechanical loading has a significant impact on the speed and efficiency of healing (Eliasson et al. 2009; Killian et al. 2012; Schepull et al. 2007; Wang et al. 2012). However, the optimal loading regime remains unclear, and the detailed mechanobiological mechanisms involved are not fully understood.

Computational approaches have been widely used in mechanobiological modelling of bone healing to enable predictions of tissue differentiation and improve the understanding of both the mechanical and biological mechanisms at play (Isaksson 2012). In order to apply this approach to tendon healing, a continuum constitutive model that can both represent the changing tendon mechanics during healing and also represent the proposed biophysical stimuli for the cells involved is required.

Continuum constitutive models developed for the quasi-static properties of tendons may be classed as either phenomenological or microstructural (Weiss and Gardiner 2001). Phenomenological models with parameters that do not provide a direct physical interpretation have successfully been used to model tendon macroscopic behaviour (Woo 1982; Woo et al. 1993; Woo 1986). However, microstructural mod-

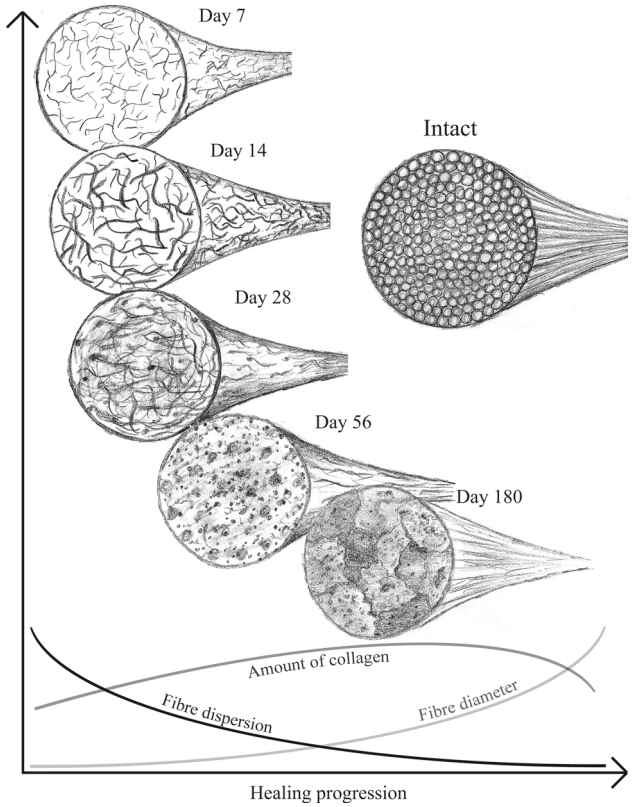

Fig. 1 Schematic structure of fibre dispersion, diameter and amount in healing tendons. Graphs illustrate patterns of changes during the healing process

els are required to capture the complex changes in density, organisation and alignment of collagen fibres during healing. With the representation of multi-scale deformation mechanisms, the complexity of such models rapidly increases, some requiring as many as seven independent parameters to be fitted (Hurschler et al. 1997; Reese et al. 2010). A compromise approach is to use some microstructural parameters that can be directly measured together with phenomenological parameters enabling a simple yet meaningful model to be analysed. Scanning electron microscopy studies in rat and rabbit models of tendon healing show how the callus develops from an isotropic gel shortly after rupture to a highly aligned, anisotropic material when healed (Fig. 1) (Sasaki et al. 2012; Enwemeka 1989). This motivates the choice of a fibre-reinforced continuum constitutive model.

One such model with distributed collagen orientations introduced by Gasser–Ogden–Holzapfel (GOH) has been widely used to simulate soft tissue mechanics (Holzapfel et al. 2000; Gasser et al. 2006). As well as extensively used to model arterial walls, this model effectively captured the link between variations in collagen arrangement and dispersion, and the tensile behaviour of the tissue in the skin dermis (Annaidh et al. 2012). It has also been used successfully to model wound healing alongside transport models for cellular and chemical species (Valero et al. 2015). To date, however, the GOH model has not been used to simulate the mechanics of healing tendons.

This study aimed to test the ability of the GOH model to capture the elastic behaviour of healing tendons using both curve fitting and a design of experiments (DOE) parametric study to examine the parameter sensitivity. Tensile test data from a rat model of Achilles tendon healing were used throughout the study (Eliasson et al. 2009).

2 Materials and methods

2.1 Gasser–Ogden–Holzapfel model

The GOH model consists of two groups of parameters—structural and phenomenological (Eq. 1; Fig. 2). The structural parameter κ represents the dispersion of the fibre alignment and γ corresponds to the alignment angle. Both can be quantified using histological or scattering methods. The phenomenological parameters $c_{10}, k_1{}'$ and $k_2{}'$ can be estimated using tensile testing (Gasser et al. 2006; Ogden et al. 2004). c_{10} represents a combination of the non-collagenous matrix neo-Hookean shear modulus and its volume fraction, whilst $k_1{}'$ and $k_2{}'$ represent a combination of the collagen fibre stiffness and collagen volume fraction. Together these are used to define the strain energy density function.

$$\boldsymbol{\Psi} = \frac{c_{10}}{2}(\boldsymbol{I}_1 - 3) + \frac{k_1{}'}{k_2{}'}\{e^{k_2{}'[\kappa \boldsymbol{I}_1 + (1-3\kappa)\boldsymbol{I}_4 - 1]^2} - 1\} \tag{1}$$

A similar scheme to that outlined by Annaidh et al. (2012) was followed to determine the constitutive parameters, assuming that the structural parameters κ and γ are known (see Sect. 2.2). To ease the calculation during the optimisation procedure, the constitutive parameters defined by Annaidh et al. (2012) were used, which are simply related to the original GOH model parameters, reported here. The data fitting was performed using the *lsqnonlin* in MATLAB with the objective function, *Err(k)* given as

$$\mathrm{Err}(k) = \sum_{i=1}^{n} (y_i^{\mathrm{exp}} - y_{\mathbf{i}}^{\mathrm{model}(k)})^2 \tag{2}$$

where n is the number of experimental data points, y_i^{exp} is the experimentally measured value of the stress of a tensile tested sample (Eliasson et al. 2009) and $y_i^{\mathrm{model}(k)}$ is the stress predicted by the model using the current set of material parameters, k. The determinant of coefficient, R^2, was used to gauge the goodness of fit. To ensure that the fits were global rather than local minima, a large range of initial parameters

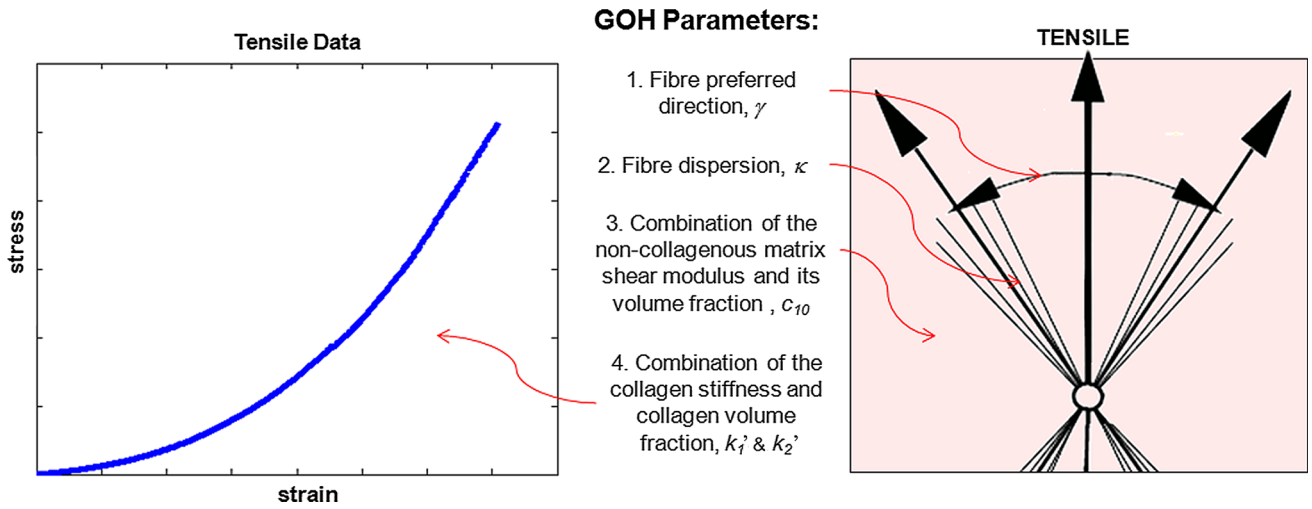

Fig. 2 Parameters of the GOH model. Please note that γ was set to zero in this study

values was manually tested, i.e. plus minus 200 % with 10 % step size. We hypothesised that the fitted values are of global mimima if they were strictly independent of initial values.

This scheme was used to fit uniaxial tensile force-displacement data from a rat Achilles tendon healing model characterising the callus at 3, 8, 14 and 21 days after transection and in intact tendons ($N = 4$–5 in each group) (Eliasson et al. 2009). The fit was performed to data with force greater than 0.5 N up to the point of rupture, which was determined at the maximum gradient.

2.2 Selection of structural parameters

The structural parameters were defined based on the literature. Collagen fibres are primarily found axially aligned throughout tendons (Wang 2006), so the alignment angle γ was set to 0°. Following scanning electron microscopy studies of healing tendons (Sasaki et al. 2012), we assumed that the alignment dispersion, κ, should decrease during healing. We defined the absolute values within the range of 0.33 to 0.00 for κ set by Gasser et al. (2006), using three criteria based on the assumed direction of change of the constitutive parameters during healing. The fibre stiffness parameters, k_1' and k_2', should increase over healing, as both more collagen is formed and the collagen crosslinks increase during repair (Fessel et al. 2012). The neo-Hookean shear modulus of the non-collagenous matrix, c_{10}, will reduce as the matrix volume fraction reduces during healing (Guo et al. 2007). Based on these premises, comparative analyses were performed between different ranges of κ. We found that the value of 0.25, 0.24, 0.23, 0.22, 0.00 for samples of days 3, 8, 14, 21, intact, respectively, produced values that generally meet the criteria above. These values were used throughout the study.

2.3 Finite element representation

The ability of the GOH model to simulate tendons undergoing repair was further tested in an axisymmetric finite element (FE) environment, assuming a perfect cylindrical shape. Five sample-specific axisymmetric models, one per timepoint (days 3, 8, 14, 21 post-rupture and intact), were created. To choose one (out of five) tendon that was representative for each time point of healing, the sample with the median R^2 value from fitting of the 1D data was selected.

The dimensions and the optimised values of the GOH parameters for each model are given in Table 1. Please note that the lengths of the models were half of the original tissues as FE analyses were performed using symmetry boundary conditions. Reduced integration hybrid rectangular axisymmetric (CAX8RH) elements were used to mesh all models. The boundary conditions from the experimental tensile test were mimicked by constraining all translational and rotational degrees of freedom of the nodes on the top edge and applying the force to the same nodes (Fig. 3). The other two edges—xsymm and ysymm—which indicate the symmetrical line of the model, were constrained in each particular direction. The model was run as a static analysis in ABAQUS/Standard (v6.12-4, Dassault Systèmes, France) with nonlinear geometry, using the NLGEOM to account for large deformations of the tendon. The values of engineering strain were compared with the experimental data, and the corresponding R^2 value was calculated.

2.4 Parametric study

A design of experiments approach based on fractional factorial designs was used to investigate the importance of the GOH parameters for characterising the mechanical behaviour of

Table 1 Parameter values and input used in the finite element analysis

Group	κ	k_1'	k_2'	c_{10}	Loading force (N)	Dimension (mm)	
						Length	Radius
Day 3	0.25	1.110	5.802	0.1669	3.3	6.0	1.2
Day 8	0.24	1.915	13.864	0.0807	14.1	8.5	1.6
Day 14	0.23	2.271	7.077	0.1791	36.5	8.4	1.8
Day 21	0.22	1.238	3.870	0.1066	31.0	7.0	1.9
Intact	0.00	9.127	1.600	4.60e−4	29.9	3.5	0.6

The values of the GOH parameters were obtained from an optimisation procedure, whilst data for model dimensions and loading, right before microfailure during tensile test were taken from Eliasson et al. (2009)

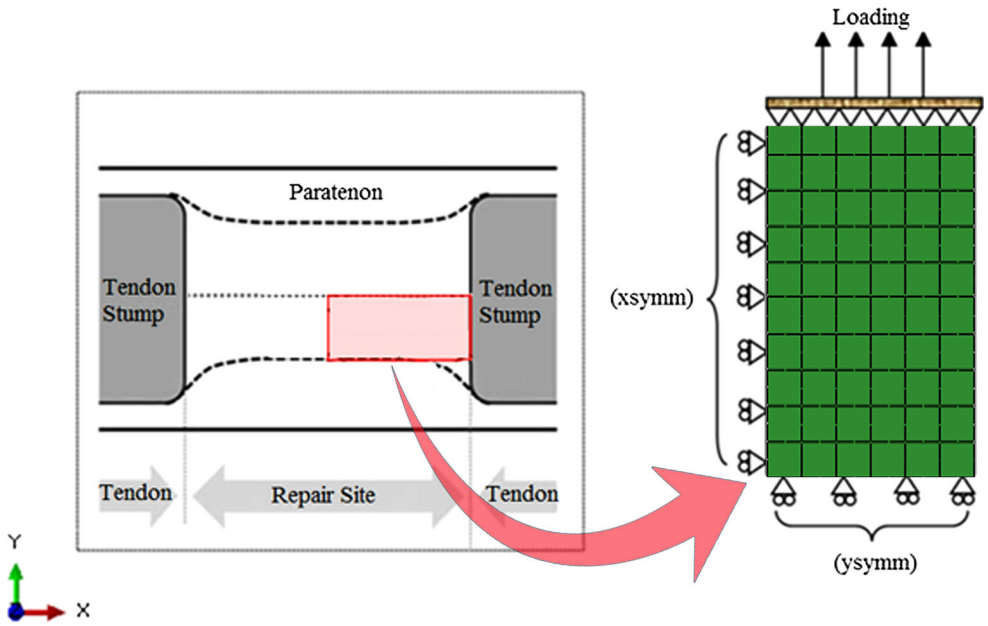

Fig. 3 Dimensions of the simulated tendon (axisymmetric). xsymm and ysymm indicate that these edges are the symmetrical line of the body with respect to its corresponding axis and are constrained in that particular direction. For instance, the xsymm edge was constrained in the x direction, which only allows the body to move in the y direction

healing Achilles tendons (Isaksson et al. 2008, 2009b). Fractional factorial designs are experimental designs that consist of carefully chosen subsets or fractions of the experimental runs needed to complete full factorial designs (Montgomery 2006; Phadke 1995). Hence, they present an efficient method to study the effects of two or more factors on a specific process. For this study, a three-level central composite design (CCD) was chosen. CCD is a type of fractional factorial design that uses a second-order model for the response surface without needing to use a complete three-level factorial design (Funkenbusch 2005; Isaksson et al. 2009b). The four GOH parameters were examined—k_1', k_2', c_{10} and κ—and are referred to as control factors, whilst the values they take are called levels. Each combination of control factor levels that is evaluated is called a treatment condition (Isaksson et al. 2008; Phadke 1995). The chosen parameter space was based on the variances of the optimised values. The low (−1) and high (+1) levels at each timepoint were set according to the variation in the experimental data as two standard deviations from the mean value. The mean value was taken as the normal (0) (Table 2). The experiment included a total of 31 treatment conditions at every timepoint of healing.

To assess the results obtained from the parametric study, criteria that characterise the performance of the system for each treatment condition were determined. A match target of 1 was set for the coefficient of determination, R^2. Analysis of variance (ANOVA) was used to calculate the normalised percentage of the total sum of squares for each factor, %TSS to measure the contribution of each factor at specific timepoints of healing (Dar et al. 2002; Isaksson et al. 2009).

Table 2 Parameter space for the DOE

Group	Levels		
	−1	0	1
	k_1'		
Day3	0.6125	1.3599	2.1073
Day8	0.9270	2.0059	3.0847
Day14	0.0001	2.8760	6.3391
Day21	0.3247	1.4412	2.5577
Intact	4.2104	11.5907	18.9710
	k_2'		
Day3	0.0001*	8.6435	25.8065
Day8	0.0001*	8.0924	16.8297
Day14	2.9620	5.8215	8.6809
Day21	1.1823	4.8871	8.5918
Intact	0.0001*	3.2600	8.7982
	c_{10}		
Day3	0.0898	0.2007	0.3115
Day8	0.0269	0.1026	0.1783
Day14	0.1141	0.1773	0.2405
Day21	0.0475	0.1057	0.1638
Intact	2.11e−4	5.83e−4	9.55e−4
	κ		
Day3	0.22	0.25	0.28
Day8	0.21	0.24	0.27
Day14	0.20	0.23	0.26
Day21	0.19	0.22	0.25
Intact**	0.00	0.03	0.06

* This number was chosen as values of the parameters must always be positive

** The assumed normal (level 0) value for the κ for intact sample is 0.00 not 0.03. As its values must always be positive, we chose 0.00 to be the low boundary instead, assuring a broadened positive parameter space

3 Results

3.1 Optimised constitutive parameters

Using the parameter ranges described, it was possible to obtain excellent fits for the GOH model for all samples at all timepoints ($0.9903 < R^2 < 0.9986$) (Fig. 4). The means of the optimised values for the constitutive parameters, k_1' and c_{10}, show the expected trends over the healing period, with the values of k_1' generally increasing, whilst c_{10} is decreasing (Table 3). A small drop in k_1' at day 21 was observed. k_2' appears to reduce over healing, contrary to expectations. The standard deviations of each parameter show the level of variability, with the average coefficients of variation, CV% of 37, 60 and 28 % for k_1', k_2' and c_{10}, respectively.

3.2 Finite element simulations

The finite element studies employing the GOH constitutive model with parameters determined from the optimised values through data fitting showed that the fits remain good ($0.9924 < R^2 < 0.9964$) (Fig. 5).

3.3 Parametric study

All parameters related to the collagen fibres were found to be highly influential, the parameters describing the dispersion, stiffness at small strain and stiffening behaviour at large strain of the collagen fibres, κ, k_1', and k_2', respectively (Fig. 6). The parameter associated with the non-collagenous matrix, c_{10} was found to be least influential. The importance of two parameters varied during the healing: the importance of the fibre dispersion, κ, was higher during early part of healing and decreased towards the end of the healing and in the intact sample. On the contrary, the small strain fibre stiffness, k_1', increased its influence gradually over healing and was more important in the intact sample.

4 Discussion

To the best of our knowledge, no previous studies have used the GOH constitutive model to simulate the mechanical behaviour of tendons at various stages of healing. We have shown that good fits ($R^2 > 0.99$) could be obtained against experimental data from intact tendons and tendons at four different timepoints of healing. Our parametric study showed that the relative importance of the collagen fibre-related GOH parameters somewhat varied during healing, but always remained well above the importance of the non-collagenous matrix parameter.

This study proposes the use of the dispersion of the collagen fibre angular distribution in the GOH model, κ, to characterise the tissue maturation during tendon healing. The reduction in collagen fibre dispersion during healing is evidenced qualitatively by electron microscopy of tendon healing in a rat model (Sasaki et al. 2012). Previously, the GOH model was used together with a quantitative method to measure fibre dispersion to fit the anisotropic properties of skin dermis (Annaidh et al. 2012). Measured fibre dispersions ranged from 0.0924 to 0.1698, which is somewhat lower than the maximum limit of 0.33. Recently, the GOH model, with a fixed fibre dispersion of 0.1404, was used to model wound healing (Valero et al. 2015). However, since there are still no quantitative measurements of collagen dispersion through tendon healing, the dispersion values in the present study were chosen to vary from 0.25 to 0.22 to simulate the reduction of the fibre dispersion in the early stage of healing tendons. This range may seem a

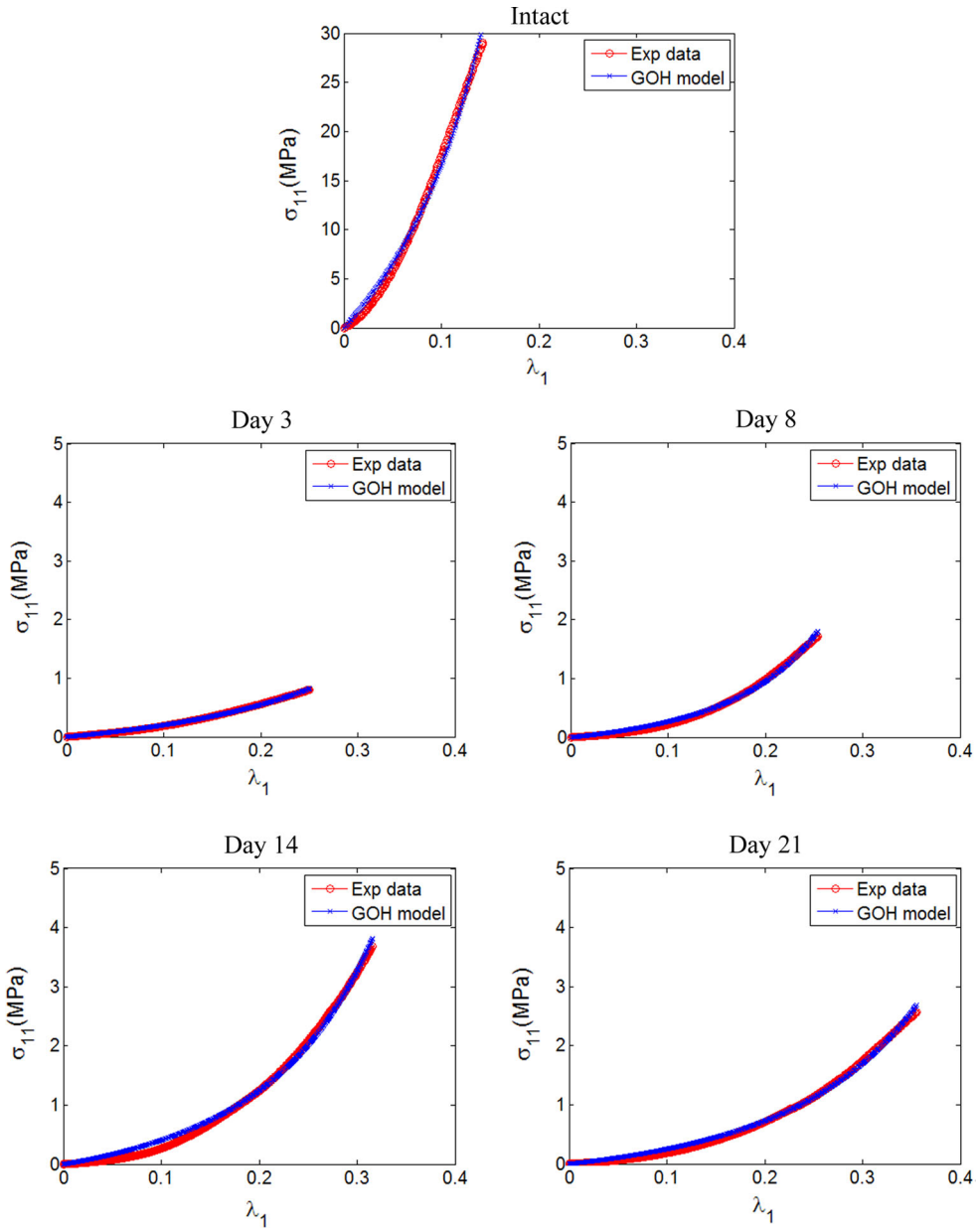

Fig. 4 Optimisation procedure of the GOH model against experimental data. Data fitting was based on the sample with the median R^2 value at each specific timepoint over healing, as representative of other samples

Table 3 The optimised model parameters for each group

Group	k_1'			k_2'			c_{10}		
	Mean	SD	CV (%)	Mean	SD	CV (%)	Mean	SD	CV (%)
Day 3	1.36	0.37	27.5	8.64	8.58	99.3	0.20	0.06	27.6
Day 8	2.01	0.54	26.9	8.09	4.37	54.0	0.10	0.04	36.9
Day 14	2.88	1.73	60.2	5.82	1.43	24.6	0.18	0.03	17.8
Day 21	1.44	0.56	38.7	4.89	1.85	37.9	0.11	0.03	27.5
Intact	11.59	3.69	31.8	3.26	2.77	84.9	5.83e−4	1.86e−4	31.9

The mean (of the samples at each group), the standard deviation (SD) and the coefficient of variation (CV) for each parameter and group are calculated

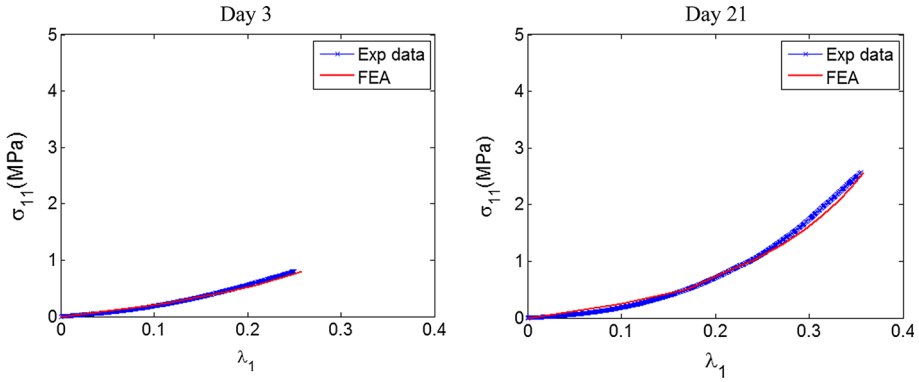

Fig. 5 Comparison between predicted model response using finite element analyses and experimental tensile data of a healing tendon at day 3 and day 21. The R^2 values were 0.9964 and 0.9959, respectively

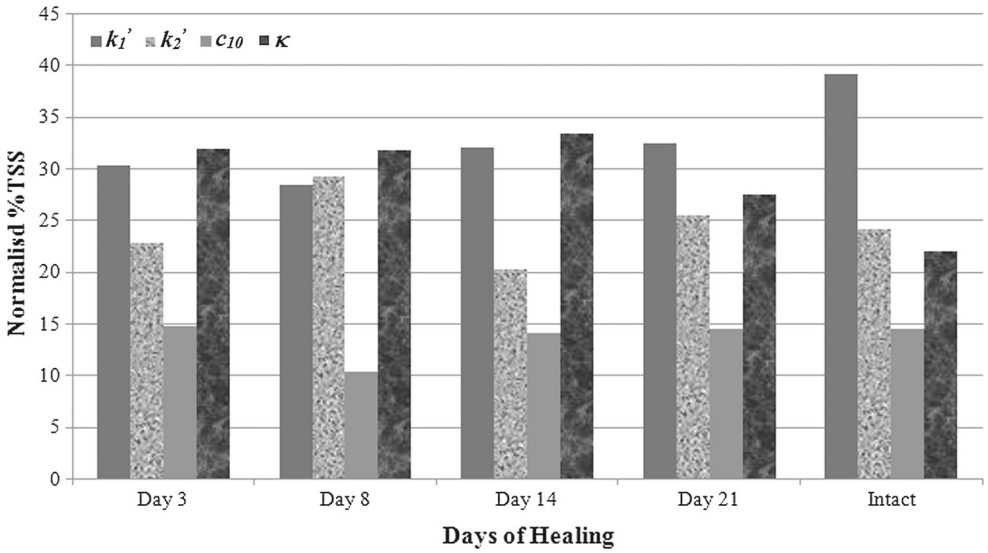

Fig. 6 ANOVA of each of the outcome variables based on the normalised %TSS

little narrow, but it has been analysed ensuring that the resulting optimised values follow the reported literature findings. On that note, we have confirmed that this setting produced k_1' values that generally increased with healing progression. However, in agreement with a drop in reported modulus of elasticity at day 21 (Eliasson et al. 2009), k_1' decreased at this timepoint compared with day 14. Eliasson et al. speculate that this decreased stiffness might be associated with upregulated tendon-specific genes also observed at this timepoint. On a general note, whilst the structural parameters in the GOH model may be directly measured in experiment, the phenomenological parameters represent a combination of volume fraction and material property that cannot be measured directly. The changes in the estimated values of these parameters over time therefore reflect changes in both material property and tissue composition.

It is well documented that the elastic modulus of healing tendons increases over time (Eliasson et al. 2009; Schepull and Aspenberg 2013; Schepull et al. 2007). The present study obtained excellent fits of the GOH model at each timepoint, with the collagen fibre stiffness, k_1' increasing during healing. The neo-Hookean shear modulus of the non-collagenous matrix, c_{10}, reduced as healing progressed, as expected. These phenomenological parameters show expected trends over time but do not change monotonically. However, k_2' showed unexpected decreases. These are phenomenological parameters, and their non-monotonic and unexpected changes are likely due to the combined influence of changes in material property, callus volume and composition.

Most of the previous continuum models of tendon were developed by assuming the tissue is similar to other soft tissues, e.g. ligament and arteries, especially when describing its time and rate independent elastic behaviour (Weiss and Gardiner 2001). An exponential stress–strain relationship based on uniaxial experiments was used by Fung (Fung 1967) to construct a phenomenological model of rabbit mesentery. This model has been widely used in capturing other soft tissues' macroscopic mechanical behaviour (Demiray 1972), e.g. arteries (Chuong and Fung 1983), cartilage (Zopf et al. 2015). However, it lacks structural information and the

model parameters are not determined via experimental data (Holzapfel et al. 2004).

Previous models to simulate microscale behaviours of tendons have been focused on collagen fibrils and their crimp pattern. Micromechanical models of helical superstructures successfully predict nonlinear behaviour and large Poisson's ratios in ligaments and tendons (Reese et al. 2010; Shearer 2015). Various other approaches including shear-lag models (Szczesny and Elliott 2014) have been implemented successfully; however, the experimental information required for their use in healing tendon is lacking. Further, this form of microstructural approach is difficult to implement in a finite element analysis.

Many modelling endeavours have shown the relevance of multi-structural fibre-reinforced constitutive models for understanding the relationship between constituents and the overall mechanical behaviour of tissues. The simplest such model is an isotropic solid matrix containing one family of fibres that has been used successfully to simulate the behaviour of fascia lata and tendons (Natali et al. 2005; Weiss et al. 1996). Another study used two distinct families of fibres to model the interwoven collagen of cruciate ligaments (Hirokawa and Tsuruno 2000). This approach was used by Holzapfel et al. in their early model development for the arterial wall (Holzapfel et al. 1996; Holzapfel and Gasser 2001). They later introduced a scalar to represent symmetrical fibre dispersion, κ (Gasser et al. 2006), allowing both the alignment and the organisation of fibres in the tissue to be represented. The very recent non-symmetrical dispersion model (Holzapfel et al. 2015) may provide an improvement over the symmetrical version used here, provided that sufficient histological information is available.

This is the first study to investigate the importance of parameters in a constitutive model of healing tendons using the design of experiment (DOE) method. DOE has been used previously in mechanobiological studies of bone healing (Isaksson et al. 2008, 2009). Our findings showed that the GOH parameters relating to collagen fibres are the most influential in characterising the tensile behaviour of healing tendons, compared to those associated with the non-collagenous matrix. This agrees with a picture of tendon healing in which the major mechanical changes over time are defined by the initial production of disorganised collagen III, and its gradual remodelling and replacement by organised collagen I. It is also noteworthy that the outcome of the parametric study reflects the experimental setup that was used. In our case, data from static tensile tests were used, which supported the hypothesis that collagen fibres are the main load-bearing components in tendons. A study by Khayyeri et al. (2015) has shown that the contributions of tendons' constituents depend upon the type of mechanical behaviour that is being analysed. For instance, in addition to the finding that collagen fibres are the main load bearer during tensile loading, they have found that repetitive tensile loading affected their viscoelastic response.

Our use of fractional factorial design of experiments with ANOVA reduces the number of computational analyses required from full factorial and gives more statistical power. Since our R^2 values, which correspond to the proportion of the variability in the data explained by the ANOVA, are all in the range of 77–92 %, the ANOVA model seems to provide a good representation of the computational model. An improved fit may be obtained with a phenomenological constitutive model of increased complexity; however, it would lack the physical relevance of GOH. Other factors that are worth considering for better fits include water content variability during healing (Oakes 2003; Sharma and Maffulli 2006). It was reported that the content was high in the early stage of healing, and later reduced to its normal state to assist the maturation of scar tissue. Also, a model that formulates collagen variability and cellular activity during healing is expected to provide a more realistic representation, as these occurrences have been pronouncedly demonstrated in a study by Wu et al. (2010).

Another limitation is that the MATLAB optimisation scheme used (*lsqnonlin*) in the current study is sensitive to the initial values and can potentially identify local minima rather that the global one. This was controlled by manually testing all the fits with a large range of initial parameter values. They all resulted in the same final fitted values, and thus we were fairly certain that identified values were of the global minima. However, other nonlinear and constrained optimisation schemes should be tested in the future to ensure a robust search for the global optimum.

It is noteworthy that design of experiments is highly dependent on its parameter space (Montgomery 2006). As there are no previous literature reports of the GOH model in tendon healing, we used ranges of values acquired from our own optimisation procedures. This requires the assumption that the experimental data used covered the parameter space comprehensively. The upper and lower bounds were set at two standard deviations, to ensure that the parameter space used was broad enough to avoid predetermining the experiment.

Our study has focused on the behaviour of only the healing part of the tendon and neglected any changes in adjacent regions. There are no published data on the microstructure along the length of the tendon, but such information will be essential for future mechanobiological studies of healing tendon.

In conclusion, we have shown that a well-established fibre-reinforced continuum model with distributed collagen orientations introduced by Gasser–Ogden–Holzapfel is able to simulate the mechanical behaviour of healing tendons. Good fits were obtained to mechanical tensile test data of healing tendons at days 3, 8, 14, 21 as well as the intact tis-

sue. Our work further provides support for using the GOH fibre dispersion, κ, to represent collagen fibre organisation in healing tendons and shows that this parameter, the fibre stiffness at low strain and stiffening behaviour at large strain are most important under tensile load. These findings support the future development of simulations of the mechanobiology of healing tendons.

Acknowledgments The support of the Oxford Mechanobiology Group, Oxford Solid Mechanics Group, BOTNAR Research Centre, Oxford, and Biomedical Engineering Department, Lund University, is gratefully acknowledged. We would like to thank Per Aspenberg, Linköping University, for kindly providing the experimental data used in this study.

References

Annaidh AN, Bruyère K, Destrade M, Gilchrist M, Maurini C, Otténio M, Saccomandi G (2012) Automated estimation of collagen fibre dispersion in the dermis and its contribution to the anisotropic behaviour of skin. Ann Biomed Eng 40:1666–1678

Chuong CJ, Fung YC (1983) Three-dimensional stress distribution in arteries. J Biomech Eng 105:268–274

Dar FH, Meakin JR, Aspden RM (2002) Statistical methods in finite element analysis. J Biomech 35:1155–1161

Demiray H (1972) A note on the elasticity of soft biological tissues. J Biomech 5:309–311

Eliasson P, Andersson T, Aspenberg P (2009) Rat Achilles tendon healing: mechanical loading and gene expression. J Appl Physiol 107:399–407

Enwemeka CS (1989) Inflammation, Cellularity, and Fibrillogenesis in Regenerating Tendon: Implications for Tendon Rehabilitation. Phys Ther 69:816–825

Enwemeka CS (1989) Inflammation, Cellularity, and Fibrillogenesis in Regenerating Tendon: Implications for Tendon Rehabilitation. Phys Ther 69:816–825

Fung Y (1967) Elasticity of soft tissues in simple elongation American. J Physiol Leg Content 213:1532–1544

Funkenbusch P (2005) Practical Guide to design experiments: unified modular approach. Marcel Dekker, New York

Gasser TC, Ogden RW, Holzapfel GA (2006) Hyperelastic modelling of arterial layers with distributed collagen fibre orientations. J R Soc Interface 3:15–35

Guo ZY, Peng XQ, Moran B (2007) Mechanical response of neo-Hookean fiber reinforced incompressible nonlinearly elastic solids. Int J Solids Struct 44:1949–1969

Hirokawa S, Tsuruno R (2000) Three-dimensional deformation and stress distribution in an analytical/computational model of the anterior cruciate ligament. J Biomech 33:1069–1077

Holzapfel GA, Niestrawska JA, Ogden RW, Reinisch AJ, Schriefl AJ (2015) Modelling non-symmetric collagen fibre dispersion in arterial walls 12:20150188

Holzapfel GA, Eberlein R, Wriggers P, Weizsäcker HW (1996) Large strain analysis of soft biological membranes: formulation and finite element analysis. Comput Methods Appl Mech Eng 132:45–61

Holzapfel GA, Ogden RW, Gasser TC (2004) Comparison of a multilayer structural model for arterial walls with a Fung-type model, and issues of material stability. J Biomech Eng 126:264–275

Holzapfel GA, Gasser TC (2001) A viscoelastic model for fiber-reinforced composites at finite strains: continuum basis, computational aspects and applications. Comput Methods Appl Mech Eng 190:4379–4403

Holzapfel GA, Gasser TC, Ogden RW (2000) A new constitutive framework for arterial wall mechanics and a comparative study of material models. J Elasticity 61:1–48

Hurschler C, Loitz-Ramage B, Vanderby JR (1997) A structurally based stress–stretch relationship for tendon and ligament. J Biomech Eng 119:392–399

Isaksson H, van Donkelaar CC, Huiskes R, Yao J, Ito K (2008) Determining the most important cellular characteristics for fracture healing using design of experiments methods. J Theor Biol 255:26–39

Isaksson H, van Donkelaar CC, Ito K (2009) Sensitivity of tissue differentiation and bone healing predictions to tissue properties. J Biomech 42:555–564

Isaksson H, van Donkelaar CC, Ito K (2009b) Sensitivity of tissue differentiation and bone healing predictions to tissue properties. J Biomech 42:555–564

Isaksson H (2012) Recent advances in mechanobiological modeling of bone regeneration. Mech Res Commun 42:22–31

Khayyeri H, Gustafsso A, Heuijerjans A, Matikainen MK, Julkunen P, Eliasson P, Aspenberg P, Isaksson H (2015) A fibre-reinforced poroviscoelastic model accurately describes the biomechanical behaviour of the rat achilles tendon. PLoS ONE 10:e0126869

Killian ML, Cavinatto L, Galatz LM, Thomopoulos S (2012) The role of mechanobiology in tendon healing. J Shoulder Elbow Surg 21:228–237

Montgomery DC (2006) Design and analysis of experiments. Wiley, New York

Natali AN, Pavan PG, Carniel EL, Lucisano ME, Taglialavoro G (2005) Anisotropic elasto-damage constitutive model for the biomechanical analysis of tendons. Med Eng Phys 27:209–214

Oakes BW (2003) Tissue healing and repair: Tendons and ligaments. In: Frontera WR (ed) Rehabilitation of sports injuries: scientific basis. Blackwell Science Ltd, Oxford, UK. doi:10.1002/9780470757178.ch4

Ogden RW, Saccomandi G, Sgura I (2004) Fitting hyperelastic models to experimental data. Comput Mech 34:484–502

Phadke MS (1995) Quality engineering using robust design. Prentice-Hall PTR, Englewood Cliffs

Reese SP, Maas SA, Weiss JA (2010) Micromechanical models of helical superstructures in ligament and tendon fibers predict large Poisson's ratios. J Biomech 43:1394–1400

Sasaki K, Yamamoto N, Kiyosawa T, Sekido M (2012) The role of collagen arrangement change during tendon healing demonstrated by scanning electron microscopy. J Electron Microsc 61:327–334

Schepull T, Kvist J, Andersson C, Aspenberg P (2007) Mechanical properties during healing of Achilles tendon ruptures to predict final outcome: a pilot Roentgen stereophotogrammetric analysis in 10 patients. BMC Musculoskelet Disord 8:116

Schepull T, Aspenberg P (2013) Early controlled tension improves the material properties of healing human Achilles tendons after ruptures: a randomized trial. Am J Sports Med 41:2550–2557

Sharma P, Maffulli N (2006) Biology of tendon injury: healing, modeling and remodeling. J Musculoskelet Neuronal Interact 6:181–190

Shearer T (2015) A new strain energy function for modelling ligaments and tendons whose fascicles have a helical arrangement of fibrils. J Biomech 48:3017–3025

Szczesny SE, Elliott DM (2014) Interfibrillar shear stress is the loading mechanism of collagen fibrils in tendon. Acta Biomater 10:2582–2590

Valero C, Javierre E, García-Aznar JM, Gómez-Benito MJ, Menzel A (2015) Modeling of anisotropic wound healing. J Mech Phys Solids 79:89–91

Wang JHC, Guo Q, Li B (2012) Tendon biomechanics and mechanobiology—a minireview of basic concepts and recent advancements. J Hand Ther 25:133–141

Wang JHC (2006) Mechanobiology of tendon. J Biomech 39:1563–1582

Weiss JA, Maker BN, Govindjee S (1996) Finite element implementation of incompressible, transversely isotropic hyperelasticity. Comput Methods Appl Mech Eng 135:107–128

Weiss JA, Gardiner JC (2001) Computational modeling of ligament mechanics. Crit Rev Biomed Eng 29:303–371

Woo SL (1982) Mechanical properties of tendons and ligaments. I. Quasi-static and nonlinear viscoelastic properties. Biorheology 19:385–396

Woo SLY (1986) Biomechanics of tendons and ligaments. In: Schmid-Schönbein GW, Woo SLY, Zweifach BW (eds) Frontiers in biomechanics. Springer, New York, pp 180–195

Woo SL, Johnson GA, Smith BA (1993) Mathematical modeling of ligaments and tendons. J Biomech Eng 115:468–473

Wu YF, Chen CH, Cao Y, Avanessian B, Wang XT, Tang JB (2010) Molecular events of cellular apoptosis and proliferation in the early tendon healing period. J Hand Surg 35:2–10

Zopf DA et al (2015) Biomechanical evaluation of human and porcine Auricular cartilage. Laryngoscope 125:E262–E268